Science of the Total Environment xxx (2014) xxx–xxx

Contents lists available at ScienceDirect

Science of the Total Environment

journal homepage: www.elsevier.com/locate/scitotenv

Fate of mercury species in the coastal plume of the Adour River estuary (Bay of Biscay, SW France)

Abubaker Sharif [a,1], Mathilde Monperrus [a], Emmanuel Tessier [a], Sylvain Bouchet [a], Hervé Pinaly [a], Pablo Rodriguez-Gonzalez [a,2], Philippe Maron [b], David Amouroux [a,*]

[a] Laboratoire de Chimie Analytique Bio-Inorganique et Environnement, Institut Pluridisciplinaire de Recherche sur l'Environnement et les Matériaux, UMR 5254 CNRS, Université de Pau et des Pays de l'Adour, Hélioparc Pau Pyrénées, 2 av. P. Angot, 64053 Pau cedex 9, France
[b] Laboratoire des Sciences de l'Ingénieur Appliquées à la Mécanique et au Génie Electrique, Institut Supérieur Aquitain du Bâtiment et des Travaux Publics, Université de Pau et des Pays de l'Adour, Allée du Parc Montaury, 64600 Anglet, France

HIGHLIGHTS

- Reactivity of mercury species was investigated in plume waters of the Adour Estuary.
- In situ water incubations were performed to examine transformation processes of Hg.
- A net MeHg demethylation was observed via both light induced and biotic pathways.
- The estuarine plume exhibits significant loss of MeHg and atmospheric evasion of Hg.

GRAPHICAL ABSTRACT

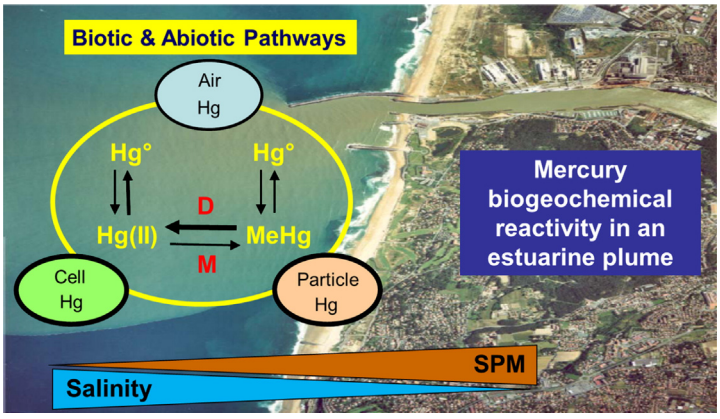

ARTICLE INFO

Article history:
Received 8 January 2014
Received in revised form 24 June 2014
Accepted 25 June 2014
Available online xxxx

Keywords:
Mercury
Speciation
Estuarine plume
Methylation
Demethylation
Reduction

ABSTRACT

Because mercury (Hg) undergoes significant biogeochemical processes along the estuarine-coastal continuum, the objective of this work was to investigate the distribution and reactivity of methylmercury (MeHg), inorganic mercury (Hg(II)) and gaseous Hg (DGM) in plume waters of the Adour River estuary (Bay of Biscay). Vertical profiles, spatial and tidal variability of Hg species concentrations were evaluated during two campaigns (April 2007 and May 2010) characterized by significant plume extents over the coastal zone. Incubations with isotopically enriched tracers were performed on bulk and filtered waters under sunlight or dark conditions to investigate processes involved in Hg methylation, demethylation and reduction rates. Total Hg(II) concentrations were more dispersed in April 2007 (5.2 ± 4.9 pM) than in May 2010 (2.5 ± 1.1 pM) while total MeHg concentrations were similar for both seasons and averaged 0.13 ± 0.07 and 0.18 ± 0.11 pM, respectively. DGM concentrations were also similar between the two campaigns, averaging 0.26 ± 0.10 and 0.20 ± 0.09 pM, respectively. Methylation yields remained low within the estuarine plume (<0.01–0.4% day^{-1}) while MeHg was efficiently demethylated via both biotic and abiotic pathways (2.3–55.3% day^{-1}), mainly photo-induced. Hg reduction was also effective in these waters (0.3–43.5% day^{-1}) and was occurring in both light and dark conditions. The

* Corresponding author. Tel.: +33 5 59 40 77 56; fax: +33 5 59 40 77 81.
E-mail address: david.amouroux@univ-pau.fr (D. Amouroux).
[1] Present address: Sebha University, Sebha, Libya.
[2] Present address: Department of Physical and Analytical Chemistry, Faculty of Chemistry, University of Oviedo, Spain.

http://dx.doi.org/10.1016/j.scitotenv.2014.06.116

results suggest that the plume is overall a sink for MeHg with integrated net demethylation rates, ranging from 2.0–3.7 g (Hg) d^{-1}, in the same range than the estimated MeHg inputs from the estuary (respectively, 0.9 and 3.5 g (Hg) d^{-1}). The large evasion of DGM from the plume waters to the atmosphere (8.8–26.9 g (Hg) d^{-1}) may also limit Hg_T inputs to coastal waters (33–69 g (Hg) d^{-1}). These processes are thus considered to be most significant in controlling the fate of Hg transferred from the river to the coastal zone.

1. Introduction

Coastal ecosystems are highly productive and ecologically rich zones due to large and continuous continental inputs of nutrients and organic matter. However, they are also exposed to various pollutants, such as metals transported by fresh water run-off from their watersheds and anthropogenic discharges due to extensive urban development along coastlines. Among metals, Hg is of special importance since it strongly accumulates in biota, leading to human and wildlife exposure. Estuaries provide a link between the marine and terrestrial environments, therefore understanding the behaviour and fate of Hg in estuaries and adjacent coastal areas has implication for larger scale Hg marine biogeochemical cycles (Fitzgerald et al., 2007). Most studies on the fate of Hg during fresh-saltwater mixing have focused on estuaries in river channels, and not considered reactions occurring in plumes as they extend out into the coastal ocean. Indeed, after rainstorms or snowmelt events, high flow water discharges of lower salinity and density form a surface-layer plume with a characteristic shape influenced by several forcing parameters such as topography, wind and tide. Plumes differ from marine waters by their high concentrations of suspended particulate matter (SPM), which are associated with nutrients, pollutants, bacteria and diverse materials, depending on the geological nature and anthropogenic activities present in the watershed.

The distribution of Hg species in the estuarine and plume waters results from their transport from the watershed and subsequent partitioning and transformations. The transport efficiency is dependent on the species distribution between the aqueous and solid phases (Choe et al., 2003; Coquery et al., 1995; Mason et al., 2012) for which the concentration and quality of dissolved and particulate organic matter is essential owing to its binding capacities (Dittman et al., 2010; Schuster et al., 2008; Shanley et al., 2008). As with Hg(II), MeHg may originate from the watershed or local discharge but it may also be produced in the downstream section. Estuarine and coastal sediments are known as active sites of MeHg production with a significant export to the water column (Monperrus et al., 2007b; Rodríguez Martín-Doimeadios et al., 2004; Schäfer et al., 2010) while Hg transformation potentials have never been reported in estuarine or plume waters. However, variations in bacterial communities between fresh and seawaters have been observed in the Adour estuary (Goni-Urriza et al., 2007) and may affect the Hg species transformations in the estuary and in the plume. It is already known that MeHg demethylation occurs simultaneously to Hg(II) methylation in the water column and is often overwhelming it since it can proceed via a biological or a photochemical route (Chen et al., 2007; Heyes et al., 2006; Tsui et al., 2013; Whalin et al., 2007). Alternatively, Hg(II) can be reduced to elemental mercury (Hg^0) usually leading to its evasion to the atmosphere. Hg reduction by bacteria was reported in the Pacific Ocean (Mason and Fitzgerald, 1991), estuarine and lake environments (Mason et al., 1995; Poulain et al., 2004). Siciliano et al. (2002) have found that phytoplankton can also reduce Hg. A better understanding of Hg species in the coastal zone requires a deeper examination of the processes leading to Hg species transformations in waters and associated rate constants. A significant number of studies have provided such data in temperate and marine environments (e.g., Coquery and Cossa, 1995; Cossa et al., 2011; Kotnik et al., 2007; Mason et al., 2012; Mason et al., 2001) while few are available for coastal environments (e.g., Balcom et al., 2008; Conaway et al., 2003; Stoichev et al., 2006).

Although Hg cycling has been intensively investigated in various inner estuaries, the fate of Hg species has not yet been studied in the plume waters. The Adour River estuary (south Gulf of Biscay) is an important French mesotidal estuary, which is highly urbanized and heavily industrialized (e.g., wood treatment chemicals, food processing, iron and steel industries). Its contamination originates from upstream rivers and from urban and industrial discharges in the lower section (Point, 2004; Stoichev et al., 2006). Although the Hg contamination level in the Adour estuary is not alarming, relatively high levels of MeHg were found in both its sediments and biota (RNO, 1999, Point, 2004, Stoichev et al., 2004, Monperrus et al., 2005, Arleny et al., 2007). Fine particles expulsed from the Adour estuary represent a major source of Hg for superficial coastal and shelf sediments along the Basque Coast (RNO, 2005; Stoichev et al., 2004). The specific hydrodynamic of the Adour estuary promotes the formation of a large plume during flood events, which results in an efficient transport of matter to the adjacent coastal zone (Petus et al., 2010). The aim of this work was therefore to investigate the distribution and biogeochemical reactivity of Hg species (MeHg, Hg(II), Hg^0) in the coastal waters impacted by the Adour River (Bay of Biscay, South of France) subsequently to typical high-flow events. The spatial and temporal variability of Hg species concentrations and transformation potentials in surface waters (methylation, demethylation and reduction) were investigated along hydrogeochemical gradients to infer the most significant pathways controlling the fate of Hg in the coastal plume.

2. Materials and methods

2.1. Study site

The Adour estuary is a mesotidal system, located in the Southwest of France, which discharges into the Bay of Biscay, Atlantic Ocean (Fig. 1). The tidal amplitude ranges between 2 and 5 m while the mean annual water discharge is about 300 $m^3 s^{-1}$ but can reach 2000 $m^3 s^{-1}$ during brief flood events. The estuarine channel is narrow with a width of about 500 m down to only 200 m at the mouth of the estuary. The upstream part of the estuary flows through agricultural areas, while the downstream part is situated within an urban and industrial area. Due to a moderate marine influence, the residence time of water and particles in the Adour Estuary is shorter (from hours to a few days) than other estuaries having a stronger marine influence (e.g., the Gironde and Scheldt Estuaries, from 30 to 90 days), (Petus et al., 2010; Point et al., 2007; Stoichev et al., 2006). However, Point et al. (2007) estimated that 75% of the annual flux of suspended solids is exported to the ocean during flooding which accounts for 30–40 days over the year.

2.2. Sampling campaigns and strategies

Water samples were collected on board the RV 'Côte de la Manche' (CNRS/INSU) during the usual spring flood period (08–12 April 2007) following stormy rain events and during seasonal snowmelt in the Pyrenees Mountains (15–20 May 2010). Hereafter the two campaigns are referred as M2-0407 and M3-0510, respectively. Four sampling stations were selected to perform vertical profiles along a salinity gradient (Fig. 1) running from the inner estuary to marine waters during both campaigns. Surface waters were collected from 10 additional stations during M2-0407 to evaluate the spatial variability.

Physical factors influencing the plume shape (e.g., river discharge, wind speed/direction and current velocity) were estimated for both campaigns. The Adour discharge into the estuary is the sum of five

Please cite this article as: Sharif A, et al, Fate of mercury species in the coastal plume of the Adour River estuary (Bay of Biscay, SW France), Sci Total Environ (2014), http://dx.doi.org/10.1016/j.scitotenv.2014.06.116

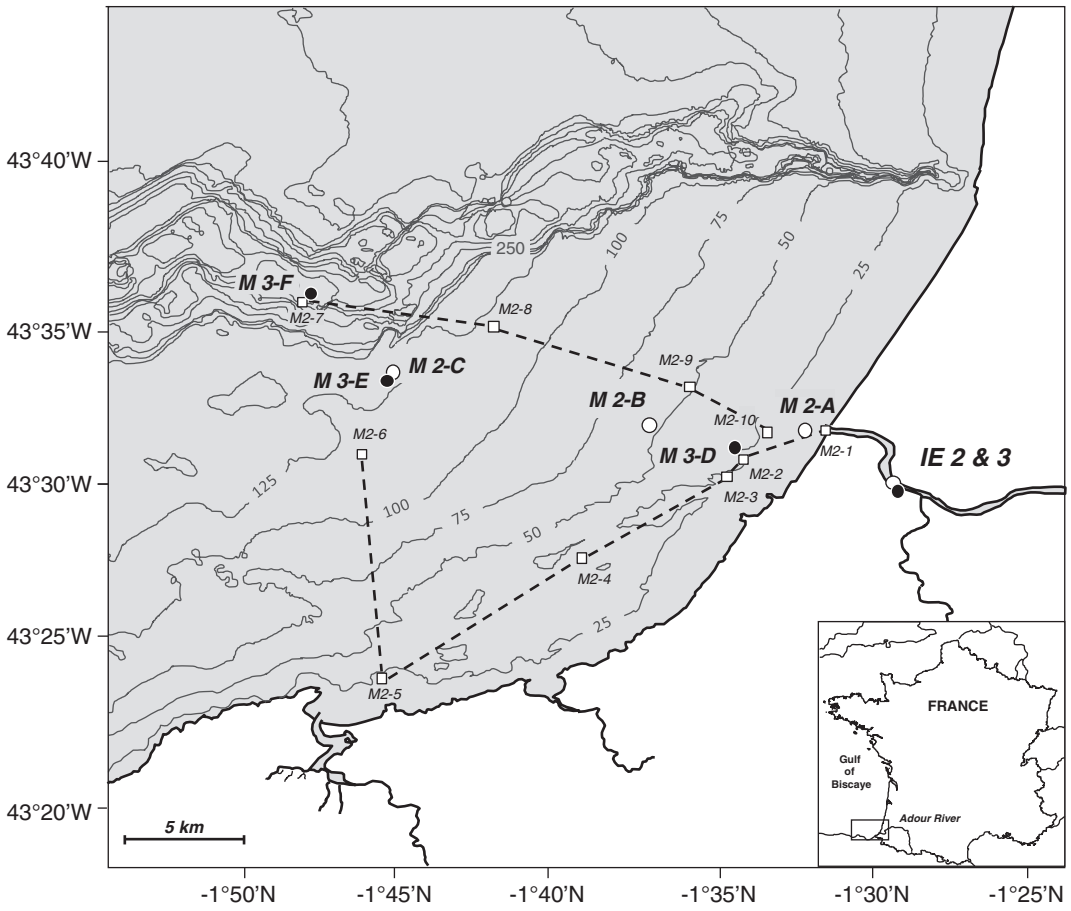

Fig. 1. Sampling locations for M2-0407 (open circles, IE-2, M2-A, M2-B, M2-C) and M3-0510 (closed circles, IE-3, M3-D, M3-E, M3-F), The dashed lines and open squares (M2-1 to M2-10) describe stations selected for a salinity gradient survey performed during M2-0407 where only surface waters (~1 m depth) were sampled.

effluent discharges (the Nive, the Bidouze, Gave de Pau, Gave d'Oloron and the Luy), which were provided by the Department of Flood Prevention of Pau (DIREN database). Satellite pictures (Fig SI-1) provided by the MarCoast/Ifremer satellite images server (MODIS satellite, URL: http://www.ifremer.fr/nausicaa/marcoast/index.htm) were used to estimate the magnitude of plume areas during both campaigns (M2-0407 and M3-0510). The suspended particulate matter (SPM) concentrations presented a dispersion pattern characterized by a concentrated plume with SPM higher than 2 mg L^{-1} and a diluted plume with SPM between 1 and 2 mg L^{-1}. It has been previously demonstrated that satellite-derived SPM concentrations generally agreed closely with *in situ* values (Petus et al., 2010), which were also checked during our campaigns. As a consequence, the discrimination of the concentrated, diluted plume and marine waters (<1 mg L^{-1} SPM) was made according to SPM concentrations and along with the salinity gradient. Wind speed and wind direction datasets were obtained from METEOGALICIA (URL: http://www.meteogalicia.es/web/index.action). Mean values of daily total solar radiation for the closest point to our sampling stations (Anglet) were obtained from Météo-France (URL: http://france.meteofrance.com).

2.2.1. Surface and depth profile water sampling

Conductivity and temperature profiles were first obtained by a CTD multi-parameter probe (Sea-Bird Electronics Inc, USA). Then, the water column was sampled at different depths ranging from 0.5–800 m for both campaigns (except IE-2) with Teflon-lined Go-Flo bottles (General Oceanics Inc, USA). Water samples were transferred from the Go-Flo bottles to 1 L Teflon bottles, which were stored in double zip-type plastic bags, and refrigerated in the dark until filtration under clean conditions (see below) within 2 hours after sampling.

2.2.2. Tidal cycle (24 h)

Water samples were collected over a tidal cycle (24 h) at two stations (M3-D and M3-E) during M3-0510, in the concentrated and diluted plume, respectively (see Fig. 1) to estimate the influence of salinity and suspended particulate matter on the concentrations of Hg species. For both stations, surface water samples (ca. 0.5 m depth) were collected every 2 h after a characterization of the water mass by CTD measurements.

2.3. Sample processing and incubation experiments

2.3.1. Incubation experiments

Incubations of surface water samples with isotopically enriched Hg species were performed for all the stations (both campaigns) within less than 2 hours after sampling. The complete protocol for water incubations, analyses and calculations of methylation (M), demethylation (D) and reduction (R) potentials has been recently described (Rodriguez-Gonzalez et al., 2013). This methodology, based on the deconvolution of isotopic pattern, provides an accurate experimental assessment of specific formation/degradation yields of Hg species. It allows simultaneous and quantitative determination of newly formed and remaining Hg species derived from each isotope, the identification of the origin of newly formed species, and the correction of isobaric interferences or instrumental mass bias (Rodriguez-Gonzalez et al., 2013). Briefly, samples were transferred directly to PFA bottles. Isotopically labelled Hg species ($^{199}HgCl_2$ and $Me^{201}HgCl$) were added at near

ambient concentrations (~12 and 1 pM, respectively) to unfiltered or filtered (0.45 μm) water samples to discriminate biotic and abiotic mediated transformations. Triplicate incubations were performed on board over a complete diurnal cycle (24 h), either exposed to sunlight or in the dark to discriminate the contribution of photochemical/photobiological factors, and temperature was regulated by seawater recirculation (Rodriguez-Gonzalez et al., 2013, Bouchet et al., 2013). Initial time (t_0) controls were obtained by adding high purity hydrochloric acid (HCl, 1% v/v) just after supplementation with the isotopic tracers. Because no Hg° oxidation rate has been measured during these incubations, we assumed that net reduction is measured at the end of the 24 hours experiments.

2.3.2. Filtration and storage of water samples

The particulate fraction (suspended matter/plankton) was collected by filtering ~ 1 L of water with Durapore® PVDF filters (0.45 μm, Millipore) under a Class 100 (ISO5) laminar flow hood on board. Each filter was rinsed with ultrapure water and immediately stored in Analyslide® Petri dish at −18 °C. Back in the lab, filters were dried at room temperature under a laminar flow hood and extracted using (6 N) pure nitric acid (HNO_3 J. T. Baker, INSTRA®) by an Explorer focused microwave system (CEM Corporation) according to previous works (Bouchet et al., 2013; Navarro et al., 2012). Filtered and unfiltered water samples were both acidified by adding 1% v/v of HCl (Ultrex® II, J.T. Baker). Filtration blanks were also performed at least each day to check the potential cross-contamination through inadequate filtration/cleaning techniques. Water samples were stored in Teflon PFA bottles at +4 °C in the dark until isotope dilution analysis by gas chromatography – inductively coupled plasma–mass spectrometry (ID-GC-ICPMS).

2.4. Analytical methods

2.4.1. Biogeochemical parameters

Suspended particulate matter (SPM), particulate organic carbon (POC), nitrate (NO_3^-), phosphate (PO_4^{3-}) and silicic acid (SiO_4^{4-}) were analyzed according to Deborde et al. (2008). POC was measured by infrared spectroscopy with a LECO C-S 125, dissolved silicate and phosphate were measured by a colorimetric method (Murphy and Riley, 1962) and NO_3^- was measured by Flow Injection Analysis (FIA), (Hall and Aller, 1992).

2.4.2. Hg speciation analysis

Mercury speciation analyses were either performed on board (DGM and total gaseous Hg, TGM) or back in the laboratory (MeHg, Hg(II)). Total Hg was calculated as (Hg_T = DGM + $Hg(II)_T$ + $MeHg_T$) assuming that other species (ethyl and phenyl Hg) were negligible. Simultaneous speciation analyses of MeHg and Hg(II) in filtered water samples (noted hereafter with "$_D$" subscript) and filter extracts (noted hereafter with "$_P$" subscript) were performed using propylation ID-GC–ICPMS as previously described (Bouchet et al., 2013), while total content of each compound (noted hereafter with "$_T$" subscript) was obtained by adding both filtered and particulate fraction concentrations. Briefly, an aliquot of 100 ml of water was accurately weighted before analysis in a headspace glass flask, spiked with known amounts and concentrations of isotopically enriched standards ($Me^{201}Hg$ and $^{199}Hg(II)$). The solution was adjusted to pH 4 by adding 5 ml of sodium acetate-acetic acid 0.1 M buffer solution and about 1 mL of concentrated ammonium hydroxide; then 250 μl of iso-octane and 300 μl (1%) of sodium tetra-propyl borate solution (1% w/v) were added for species derivatization and extraction. The vials were caped and shaken for 5 min; then the iso-octane was recovered and analyzed in triplicate by GC-ICPMS.

For the speciation of DGM, both elemental mercury (Hg^0) and dimethylmercury (DMHg) contents were determined in several samples. Hg^0 was determined for all samples on board immediately after sampling according to Bloom and Fitzgerald, 1988; Bouchet et al., 2011. Briefly, water samples were gently transferred to a 1 L glass or Teflon® purging vessel and bubbled for 1 hour with a Hg-free helium flow (c.a. 600 mL min^{-1}). The gas stream was dried through a moisture trap (ice-acetone bath at −20 °C) before cryogenic or gold trapping. Gold traps were analysed on board by AFS while cryogenic traps analyses for DMHg were carried out later by cryogenic trapping–gas chromatography–ICPMS (CT-GC-ICPMS), following the method developed by Amouroux et al., 1998. Since DMHg concentrations measured were always below detection limits in coastal waters (<1 fM), even at depth below the thermocline, we further assume that DGM represents only the dissolved Hg^0 concentration. TGM in air was sampled at 10 m above the water surface and continuously measured by an automatic 2537B Tekran® analyzer (Schroeder et al., 1995). The instrument was placed on the upper deck of the vessel and samples were taken every 5 min at a 1.5 L min^{-1} flow rate. TGM measurements were performed only during the M3-0510 campaign.

2.4.3. Hg gaseous fluxes at the air-water interface

As recently described by Sharif et al. (2013), gaseous Hg fluxes (F, pmol m^{-2} h^{-1}) were calculated using the following equation, where DGM and TGM are the concentrations of Hg0 in water and atmosphere, respectively (pmol m^{-3}), and H is the dimensionless Henry's Law constant corrected for water temperature and salinity (Bouchet et al., 2011).

$$F = k\left([DGM] - \frac{[TGM]}{H}\right) \quad (1)$$

The Hg^0 gas transfer velocity (k, m h^{-1}) at the air-water interface was computed according to the gas exchange model of Clark et al. (1995):

$$k = 2 + 0.24u_{10}^2\left[{}^{Sc_{Hg}}\!/_{Sc_{CO_2}}\right]^{-1/2} \quad (2)$$

where u_{10} is wind speed at 10 m height, *Sc* is the temperature and salinity corrected Schmidt number of Hg and CO_2 in water.

2.4.4. Quality assurance of Hg determinations

All tubing, connections and materials used for both sampling and analyses were made of Teflon® (PFA) or glass (Pyrex®) and were submitted to ultra-trace cleaning procedures including several acid washings, milli-Q water rinsing as well as drying under a laminar flow hood and conditioning in double PE ziplock bags until uses. The method detection limits (DLs) were defined as three times the standard deviation of the procedural blanks (n = 3). For ID-GC-ICPMS, DLs were 0.07 pM for MeHg and 0.13 pM for Hg(II). For CT-GC-ICPMS, DLs of Hg^0 (DGM) were 0.03 pM while for the AFS measurements (Tekran®-2537B), DLs were <0.1 ng m^{-3}. Accuracy for Hg_T was checked using certified reference material (coastal seawater, BCR®-579, IRMM Europe) and found in agreement with the certified value (1.9 ± 0.5 ng L^{-1}). All reported Hg concentrations were blank corrected.

The statistical analyses of the data were performed through Pearson linear regression using Microsoft Office Excel software (Microsoft Corporation, Redmond, WA, USA), and One way analysis of variance (ANOVA) and ANOVA post hoc (ANOVA followed by Tukeys multiple comparison procedure) using R software (R.2.14.2).

3. Results

3.1. Characterization of the plume

3.1.1. Physical forcing and stratification

Daily river discharges varied between 384 and 477 m^3 s^{-1} during the campaigns (Table 1) but it once reached up a maximum of 1150 m^3 s^{-1} (flood event on 5–10 May 2010) one week before the M3-0510 campaign (Fig. SI-2). Wind speeds were moderate, from 3 to 4 m s^{-1} during both campaigns and also reached up 10 m s^{-1} one

Please cite this article as: Sharif A, et al, Fate of mercury species in the coastal plume of the Adour River estuary (Bay of Biscay, SW France), Sci Total Environ (2014), http://dx.doi.org/10.1016/j.scitotenv.2014.06.116

Table 1
Physical and biogeochemical parameters at the different stations where vertical profiles were carried out during both campaigns (M2-0407 and M3-0510), SPM: suspended particulate matter, POC: particulate organic carbon. (n/a: not available, nd: not detected).

Stations and locations	Date	Depth	Daily River discharge	Water Temperature	Daily Radiation	Salinity	Turbidity	SPM	POC	Chlorophyll a	Phaeo-pigment	Nitrate	Phosphate	Silicic acid
		m	$m^3\ s^{-1}$	°C	$Wh\ m^{-2}$		NTU	mgL^{-1}	%	μgL^{-1}	μgL^{-1}	μM	μM	μM
Metadour 2 (April 2007) M2-0407														
IE-2 (43°30.2′N, −01°29.5′W)	11.04.2007	0.5	383.7	14.3	292	0.9	10.8	11.5	4.7	3.6	9.4	115.3	0.1	58.9
M2-A (43°31.7′N, −01°32.2′W)	08.04.2007	0.5	393.5	12.7	550	25.2	n/a	2.7	15.2	4.1	7.6	36.1	nd	8.2
		4		12.6		30.4	n/a	2.9	13.1	12.1	30.8	5.5	nd	0.9
		12		12.5		34.6	n/a	3.2	8.5	3.8	11.6	1.2	nd	1.1
M2-B (43°31.9′N, −01°37.1′W)	10.04.2007	0.5	393.9	13.5	409	25.3	1.3	3.6	12.7	5.5	14.3	20.4	nd	5.3
		2		13.1		30.2	0.8	3.2	15.2	6.5	18.6	40.8	nd	11.2
		4		12.7		32.5	0.2	1.7	19.8	9.6	29.2	6.1	0.1	1.4
		8		12.2		33.2	nd	1.4	21.3	9.3	22.0	2.4	nd	1.2
		20		12.5		35.0	nd	0.4	20.6	0.1	2.3	nd	nd	0.2
		40		12.9		35.4	nd	0.5	15.2	0.4	1.0	2.0	0.1	1.3
M2-C (43°33.5′N, −01°45.3′W)	09.04.2007	0.5	468.6	13.5	438	32.2	nd	4.6	9.9	5.1	14.2	n/a	nd	11.8
		4		13.4		34.2	nd	0.5	18.8	0.7	2.0	0.4	nd	1.1
		12		12.6		34.6	nd	0.2	36.7	0.8	2.4	0.4	0.1	1.6
		20		12.7		35.0	nd	0.3	18.8	0.7	n/a	1.0	nd	2.0
		30		12.8		35.3	nd	0.2	32.3	0.7	1.6	1.4	0.1	2.3
		50		13.0		35.6	nd	0.3	24.5	0.6	1.5	2.4	0.1	2.2
Metadour 3 (May 2010) M3-0510														
IE-3 (43°30.2′N, −01°29.5′W)	15.05.2010	0.5	476.8	12.3	235	0.2	n/a	18.9	4.6	0.5	4.2	114.1	0.2	7.3
		6		12.3		0.2	n/a	20.9	4.4	n/a	n/a	145.7	0.2	41.9
M3-D (43°31.1′N, −01°34.3′W)	16.05.2010	0.5	573.0	14.3	520	27.7	4.9	4.6	6.7	0.9	2.7	12.6	0.1	4.7
		1	452.1	14.3		27.1	4.6	4.3	n/a	0.5	2.2	15.3	0.1	7.5
		5		14.5		35.0	1.0	0.7	n/a	0.8	1.9	3.4	nd	0.5
		24		14.2		35.4	0.4	0.1	n/a	0.3	0.8	1.3	0.1	n/a
M3-E (43°33.3′N, −01°45.2′W)	17.05.2010	0.5	389.4	15.5	411	34.6	1.4	1.1	9.3	0.4	1.2	2.3	0.1	0.3
		1	452.1	15.3		31.5	1.5	1.2	n/a	1.3	2.8	1.0	0.1	nd
		4		14.8		35.2	0.4	0.1	n/a	1.3	2.8	n/a	n/a	n/a
		13		14.4		35.2	0.3	nd	n/a	0.5	1.2	0.4	0.1	nd
		20		14.0		35.6	0.1	nd	n/a	0.5	1.2	n/a	n/a	n/a
		55		13.7		35.6	0.1	nd	n/a	0.1	0.5	3.4	0.2	nd
		80		13.4		35.6	0.3	nd	n/a	0.1	0.5	n/a	n/a	n/a
M3-F (43°36.1′N, −01°47.8′W)	18.05.2010	5	412.3	14.7	724	35.2	0.3	0.7	10.0	0.4	1.2	2.4	0.1	nd
		22		14.1		35.4	0.3	0.9	10.8	0.8	2.3	7.8	0.1	nd
		40		12.5		35.6	0.1	0.8	10.4	n/a	n/a	n/a	n/a	n/a
		80		12.3		35.7	0.1	nd	n/a	n/a	n/a	n/a	n/a	n/a
		240		12.0		35.7	0.4	0.1	n/a	0.2	0.3	10.0	0.1	0.3
		800		10.7		35.7	0.5	0.1	n/a	0.1	0.2	4.4	0.2	0.1

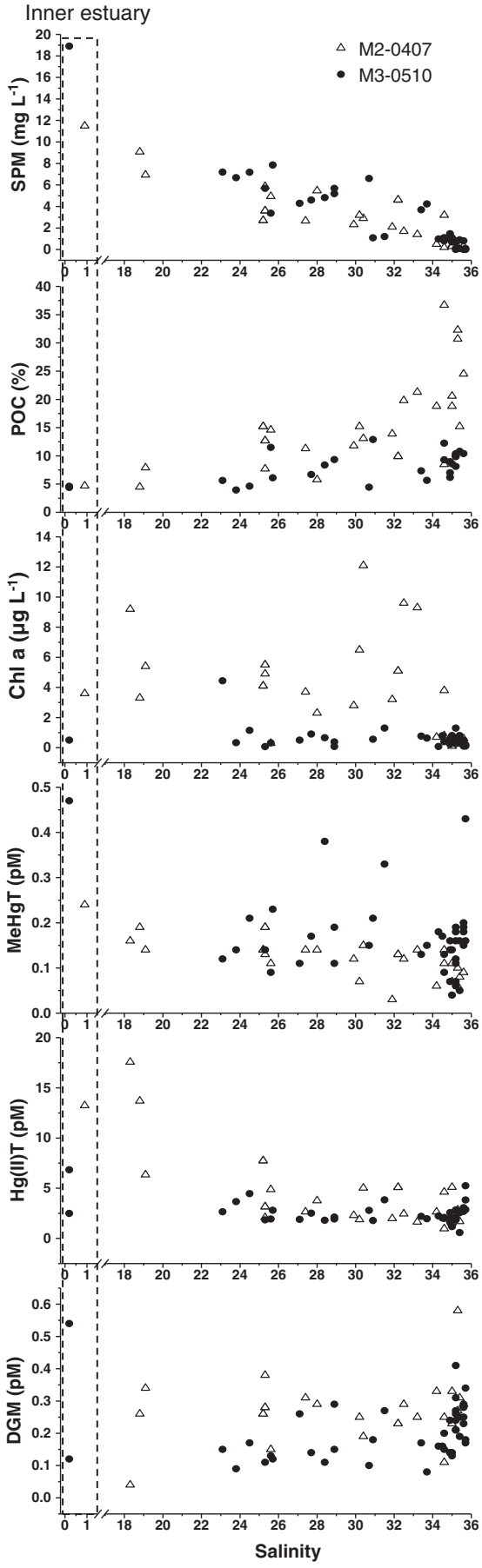

week before the M3-0510 campaign. Tidal ranges were higher during M3-0510 (2.6–3.4 m) than during M2-0407 (1.2–2.3 m). In both cases, the progressive mixing of fresh and marine waters formed large brackish plumes extending up to several tens of kilometres seaward (Fig. SI-3a&b). The most outstanding feature is the variability of the shape and areas of the concentrated and diluted plumes. For example, during M2-0407, the areas were estimated to be 274 km^2 for the concentrated plume and 119 km^2 for the diluted one. However, during M3-0510, they were only 83 km^2 and 94 km^2 for the concentrated and diluted plume, respectively, although the Adour discharge was higher.

The vertical mixing between the plume and marine waters is exemplified in Fig. SI-4 which exhibits salinity and temperature data for two stations located in the concentrated plume (M2-B and M3-D). During M2-0407, the salinity increased stepwise in the top 5 m from 25.3–32.5, showing a progressive mixing and reached a typical marine value (35.4) below 15 m, while the temperature decreased from 13.5 °C at <1 m depth down to 12.7 °C at 5 m depth and 12.5 °C at 25 m. During M3-0510, the salinity variations were smaller and increases from 27.7–35.0 between <1 and 5 m and up to 35.4 at 25 m. The temperature increased from 13.3 °C at the surface to 14.5 °C at 5 m depth in this case. The plume was more stratified during M2-0407 (max depth ≤1 m) due to rather calm weather conditions and lower tidal mixing than during M3-0510 (max depth ≥1 m) for which a higher tidal range and the storm event that occurred a few days before promoted an effective mixing of the water masses.

3.1.2. Biogeochemical characteristics

Physical and biogeochemical parameters associated to depth profiles carried out during both campaigns are presented in Table 1. Overall, coastal water temperatures (0–50 m depth) were rather homogeneous between M2-0407 and M3-0510 ranging from 12.2–15.5 °C. The salinity of surface waters was low in the inner estuary (0.2–0.9) but sharply increased at the mouth and towards the more marine stations (32.2–35.2). In contrast, the highest SPM concentrations were found in the inner estuary (11.5–20.9 mg L^{-1}) and decreased gradually to 0.7–4.6 mg L^{-1} in coastal waters (M2-C and M3-F), showing a negative trend with salinity (Fig. 2). Conversely, higher percentage of POC in suspended matter (% POC) were found with increasing salinity, ranging from 5–40% during M2-0407 and from 5–10% during M3-0510. This trend reflects the distinct origin of particulate matter in the estuary and marine waters, being mainly of biological origin in the latter case. Chlorophyll a and phaeopigments concentrations in the whole water column were found to be higher during M2-0407 (4.0 ± 3.8 and 11 ± 10 µg L^{-1}, respectively) than those found during M3-0510 (0.5 ± 0.4 and 2 ± 1 µg L^{-1}, respectively, Table 1), in relation with a larger phytoplankton biomass during the first campaign. Nitrate concentrations decreased from 114.1 µM in the inner estuary to lower than 0.6 µM in the marine waters during both campaigns. Phosphate contents were lower or equal to 0.2 µM at all the investigated locations. Silicic acid concentrations were not measured in all stations, but followed a typical trend decreasing along with increasing salinity gradient (Table 1). No relationships could be established between phytoplankton pigments and nutrients concentrations as estuarine inputs probably control nutrients load in plume waters.

3.2. Distribution and variations of Hg species concentrations

3.2.1. Hg species distribution for each campaign

Individual Hg species concentrations for both campaigns are presented in Table 2 and Table SI-1. Distributions of concentrations,

Fig. 2. Distribution of suspended particulate matter (SPM), percentage of particulate organic carbon (POC), Chlorophyll *a* (Chl.a) and Hg species; total methylmercury ($MeHg_T$) and inorganic mercury ($Hg(II)_T$) along the salinity gradient in shelf waters (<50 m depth) during M2-0407 and M3-05103.

Please cite this article as: Sharif A, et al, Fate of mercury species in the coastal plume of the Adour River estuary (Bay of Biscay, SW France), Sci Total Environ (2014), http://dx.doi.org/10.1016/j.scitotenv.2014.06.116

Table 2
Summary of Hg species concentration detected in the various vertical profiles carried out during both campaigns, Hg_T = DGM + $MeHg_T$ + $Hg(II)_T$. RSD for all species are <10%.

Station	Depth	DGM	$MeHg_D$	$Hg(II)_D$	$MeHg_P$	$Hg(II)_P$	$MeHg_T$	$Hg(II)_T$	Hg_T	Hg_P/Hg_T	$Hg(II)_T/Hg_T$	$MeHg_T/Hg_T$
	M	pM			nmol g^{-1}		pM			%	%	%
Metadour 2 (April 2007) M2-0407												
IE-2 (43°30.2′N, −01°29.5 W)	0.5	n/a	0.16	1.70	0.08	11.54	0.24	13.24	13.48	86.2	98.2	1.8
M2-A (43°31.7′N, −01°32.2′W)	0.5	0.26	0.11	1.66	0.03	2.96	0.14	5.47	5.93	59.6	92.0	2.8
	4	0.19	0.10	2.22	0.05	2.81	0.15	4.23	4.43	53.2	93.5	2.9
	12	0.11	0.13	5.78	0.02	1.97	0.14	4.29	4.34	25.1	98.2	1.8
M2-B (43°31.9′N, −01°37.1′W)	0.5	0.28	0.17	1.66	0.02	1.50	0.19	3.16	3.63	41.9	87.0	5.2
	2	0.25	0.06	1.05	0.01	0.85	0.07	1.89	2.22	38.6	85.4	3.4
	4	0.29	0.11	1.73	0.01	0.72	0.12	2.45	2.87	25.4	85.5	4.3
	8	0.25	0.13	0.77	0.01	0.89	0.14	1.65	2.04	43.9	80.8	7.1
	20	0.23	0.06	0.67	0.01	0.88	0.07	1.55	1.85	48.2	83.9	3.7
	40	0.31	0.07	0.92	0.01	0.78	0.08	1.70	2.09	37.5	81.5	3.7
M2-C (43°33.5′N, −01°45.3′W)	0.5	0.23	0.09	2.94	0.04	2.16	0.13	5.09	5.46	40.3	93.3	2.5
	4	0.33	0.06	2.16	<d.l.	0.49	0.06	2.64	3.04	16.1	87.1	2.0
	12	0.25	0.11	0.65	0.01	0.33	0.11	0.97	1.33	25.0	72.8	8.5
	20	0.33	0.10	0.84	0.01	4.26	0.11	5.10	5.54	77.1	92.2	1.9
	30	0.27	0.05	1.96	0.01	0.81	0.06	2.77	3.10	26.5	89.5	1.9
	50	0.29	0.09	1.03	0.01	1.85	0.09	2.88	3.26	56.9	88.4	2.8
Metadour 3 (May 2010) M3-0510												
IE-3 (43°30.2′N, −01°29.5′W)	0.5	0.12	0.27	1.41	0.35	5.41	0.62	6.83	7.57	76.2	90.2	8.2
	6	0.54	0.22	1.32	0.26	1.17	0.47	2.49	3.50	40.7	71.2	13.4
M3-D (43°31.1′N, −01°34.3′W)	0.5	0.14	0.11	1.62	0.06	0.89	0.17	2.51	2.82	32.5	88.4	6.3
	1	0.26	0.09	1.38	0.02	0.52	0.11	1.90	2.28	23.9	83.6	4.8
	5	0.13	0.04	1.10	0.01	0.07	0.04	1.17	1.35	5.7	86.8	3.2
	24	0.19	0.05	0.49	0.01	0.09	0.05	0.58	0.82	11.2	70.5	6.4
M3-E (43°33.3′N, −01°45.2′W)	0.5	0.20	0.07	1.14	0.04	0.90	0.09	2.00	2.29	37.0	87.4	4.6
	1	0.27	0.09	0.95	0.14	2.37	0.33	3.84	4.44	56.7	86.5	7.5
	4	0.26	0.02	0.61	0.16	2.17	0.18	2.78	3.22	72.1	86.3	5.5
	13	0.31	0.04	1.08	0.07	0.96	0.11	2.04	2.47	42.0	82.9	4.6
	20	0.23	0.08	1.06	0.10	1.63	0.18	2.69	3.09	55.8	86.9	5.7
	55	0.25	0.04	1.06	0.15	1.77	0.19	2.84	3.27	58.7	86.6	5.8
	80	0.28	0.12	2.33	0.08	0.54	0.20	2.86	3.35	18.4	85.6	6.0
M3-F (43°36.1′N, −01°47.8′W)	5	0.21	0.06	1.64	0.10	1.19	0.16	2.83	3.20	40.2	88.3	5.1
	22	0.25	0.10	1.69	0.07	1.21	0.16	2.56	2.97	43.1	86.2	5.3
	40	0.29	0.11	1.82	0.05	1.23	0.15	3.06	3.50	36.5	87.3	4.4
	80	0.18	0.10	1.62	0.06	2.22	0.16	3.83	4.18	54.5	91.7	3.9
	240	0.17	0.12	1.26	0.05	3.99	0.16	5.25	5.58	72.3	94.1	2.9
	800	0.34	0.13	0.95	0.30	1.92	0.43	2.87	3.64	61.1	78.9	11.8

percentages of species in the particulate fraction or as compared to Hg_T are presented in Fig SI-5 (including all Hg data from this study). $Hg(II)_T$ concentrations ranged from 1.0–21.1 pM (average 5.2 ± 4.9 pM, n = 30) during M2-0407 and were overall higher than during M3-0510, where concentrations ranged from 0.6–6.8 pM with an average value of 2.5 ± 1.1 pM (n = 43). Those distributions mainly reflect the differences in estuarine $Hg(II)_T$ concentrations, which were higher during M2-0407 as can be seen from measurements at IE-2, M2-A and M2-1. The percentages of $Hg(II)_T$ as $Hg(II)_P$ were similar for both campaigns, although slightly higher for M2-0407 with an average of 49 ± 21% compared to 39 ± 18% for M3-0510. The contribution of $Hg(II)_T$ to Hg_T was similar during M2-0407 (90 ± 7%) or M3-0510 (87 ± 5%). $MeHg_T$ concentrations ranged from 0.03–0.39 pM (average 0.13 ± 0.07 pM) during M2-0407 compared to 0.04–0.62 pM (average 0.18 ± 0.11 pM) for M3-0510. However, the percentages of $MeHg_T$ as $MeHg_P$ were clearly lower during M2-0407 (16 ± 10%) than M3-0510 (44 ± 21%). The contribution of $MeHg_T$ to Hg_T was also lower during M2-0407 (3.2 ± 1.7%) than M3-0507 (6.1 ± 2.7%).

The range of DGM concentrations were similar during M2-0407 (0.04-0.58 pM) and M3-0510 (0.08–0.54 pM), and average values were close to each other (0.26 ± 0.10 and 0.20 ± 0.09 pM). Its contribution to Hg_T was also really similar in both cases, averaging 7.8 ± 5.0% and 7.7 ± 4.0%, respectively. Total atmospheric gaseous Hg (TGM) concentrations were continuously measured during the second campaign only (M3-0510), in order to obtain reference values to compute air-sea exchanges of Hg^0. Very homogeneous concentrations were measured with an overall average of 1.46 ± 0.07 ng m^{-3} (n = 1537, data not shown).

3.2.2. Spatial and tidal variability in surface waters

The spatial variability of Hg species concentrations in surface waters was mainly studied along a salinity/SPM gradient during M2-0407 (Table SI-1 and Fig SI-6). Maxima of Hg_T concentrations were detected at the estuarine mouth; they were found to gradually decrease towards the west and more sharply in the north-south section of the plume (Fig SI-6). This is related to the plume hydrodynamics since fresh waters from the estuary are mainly flowing westward on marine waters and dilution of this upper layer is more effective on the sides than at the front of the plume. The dilution effect of $Hg(II)_T$ is however clearly observed in Fig. 2 when plotted against salinity. The concentrations of $MeHg_T$ detected in coastal surface waters were lower than in the estuary but didn't show a pronounced dilution effect. $MeHg_T$ concentrations in the plume remain overall homogeneous along the salinity gradient, suggesting that inputs and losses of MeHg were balanced. DGM concentrations slightly increased in surface waters, from south-east to north-west, according to the salinity level.

The tidal variability of salinity, SPM and Hg species concentrations in surface waters of the diluted and concentrated plume was investigated during M3-0510 as shown in Fig. 3. In the concentrated plume (M3-D), the maximum SPM concentrations and lowest salinity were detected at low tide, as expected. The $Hg(II)_P$ concentrations and $Hg(II)_T$, which ranged from 1.81–4.46 pM, were also found highest at low tide. No clear trends could be observed with tide for $MeHg_P$ or $MeHg_T$ (0.09–0.38 pM). DGM concentrations averaged 0.14 ± 0.06 pM (0.08–0.29 pM) in the concentrated plume but were not influenced by the tide either.

Please cite this article as: Sharif A, et al, Fate of mercury species in the coastal plume of the Adour River estuary (Bay of Biscay, SW France), Sci Total Environ (2014), http://dx.doi.org/10.1016/j.scitotenv.2014.06.116

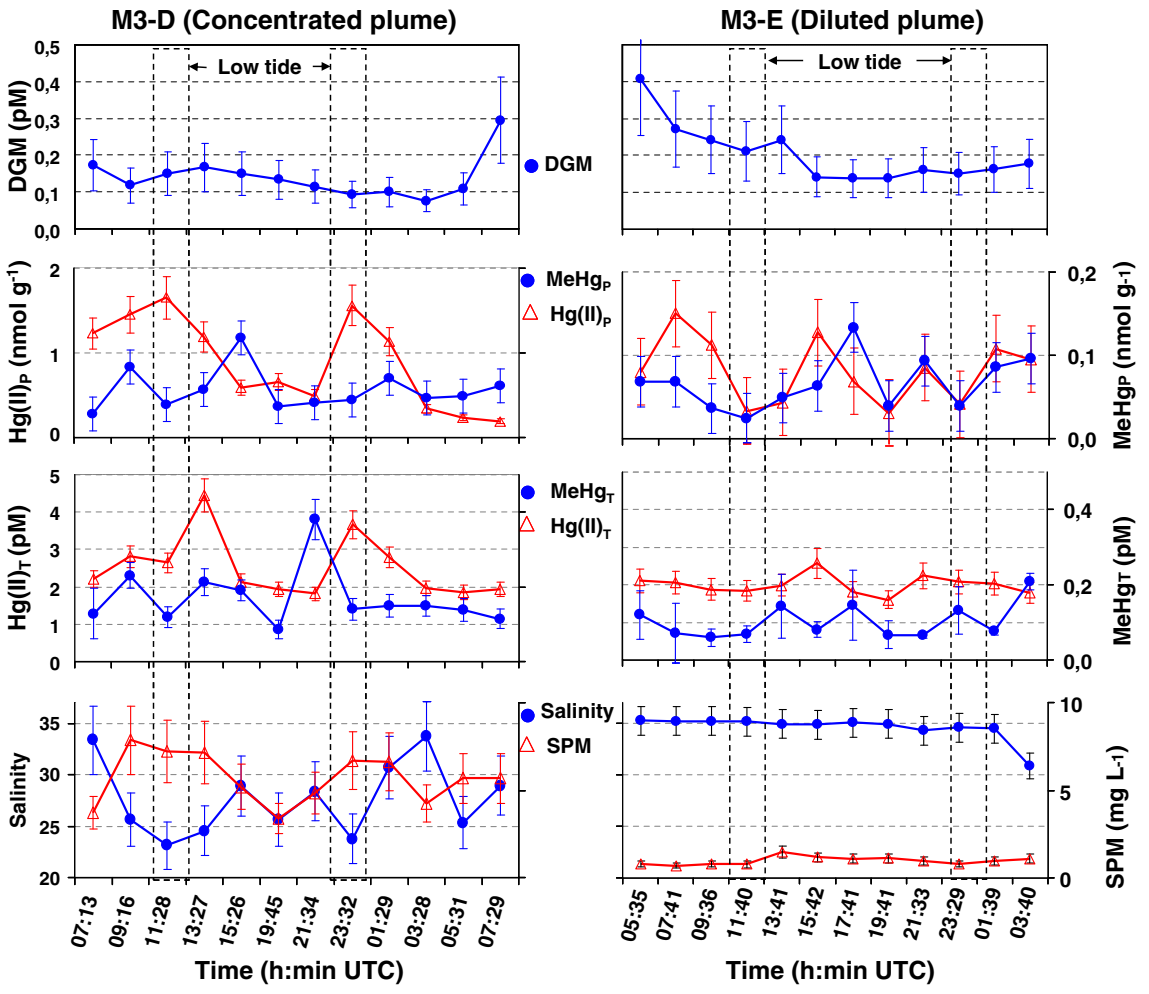

Fig. 3. Variations of salinity, SPM and Hg species concentrations throughout 24 h tidal cycles monitoring at M3-D (concentrated plume) and M3-E (diluted plume), during M3-0510.

In the diluted plume (M3-E), salinity remained constant around 35 with one low value (30.9) after the second low tide. SPM varied between 0.8 and 1.5 mg L^{-1}, roughly 5 times lower than in the concentrated plume. The concentrations of $MeHg_P$ (0.02–0.13 nmol g^{-1}) and $Hg(II)_P$ (0.3–1.5 nmol g^{-1}) were variable with lower values observed at low tide. However, the variations of the $Hg(II)_T$ (1.60–2.27 pM) or $MeHg_T$ concentrations (0.05–0.19 pM) were not so significant in this site. The DGM concentrations ranged from 0.14–0.27 pM but their evolution was independent from the tide. The variations in salinity, SPM and Hg species total concentrations (except DGM) were really restricted compared to the concentrated plume, demonstrating less influence of the tidal estuary at this point.

3.2.3. Depth profile along the Adour River plume

Two comparable stations located in the concentrated plume area (M2-B and M3-D) were selected to exemplify the vertical distribution of Hg species along with other parameters (Table 1, Fig. 4). $Hg(II)_T$ concentrations in the surface plume waters ranged from 1.90–3.16 pM at M2-B and from 1.90–2.5 pM at M3-D. Significantly lower values were detected deeper than the mixed layer (<5 m depth) with a range of 1.55-1.70 and 0.58-1.17 pM in M2-B and M3-D, respectively. Within surface plume waters (0–1 m), homogeneous distributions and significant enrichment of $MeHg_T$ were observed in both stations (M2-B and M3-D) ranging from 0.11–0.19 pM. Below the mixed layer (depth > 5 m), significantly lower concentrations were detected from 0.07–0.14 pM at M2-B and from 0.04–0.05 pM at M3-D, while no specific relationship could be obtained with the measured biogeochemical parameters. DGM concentrations were rather homogeneous with depth and similar between the two campaigns, ranging from 0.23–0.31 pM at M2-B and 0.13–0.26 pM at M3-D. Generally, higher concentrations of Hg species were detected within the first meters close the estuarine mouth while values were more homogeneous with depth towards the marine stations, indicating an effective mixing of water masses. No enrichments were observed in samples collected close to the bottom, suggesting a limited influence of benthic fluxes on Hg concentrations. This was likely since near shore surface sediments are mostly composed of coarse particles (sand) and do not present large accumulation of Hg species (Stoichev et al., 2004).

3.3. Hg species transformations in plume waters

Significant methylation yields (up to 0.4% day^{-1}, Table 3) were detected only during M2-0407 while they were always lower than the detection limit (0.01% day^{-1}) during M3-0510. The methylation yields were lower than the detection limit in filtered waters from the near shore (M2-A) and marine (M2-C) stations but could reached 0.1% day^{-1} in unfiltered waters. The higher values were found at the concentrated plume station (M2-B), in the presence of light (0.3–0.4% day^{-1}), demonstrating the importance of both light and particulate matter in the methylation process(es). To assess the statistical significance of these incubations results, one way analysis of variance (and ANOVA post hoc) was performed in order to compare both

Please cite this article as: Sharif A, et al, Fate of mercury species in the coastal plume of the Adour River estuary (Bay of Biscay, SW France), Sci Total Environ (2014), http://dx.doi.org/10.1016/j.scitotenv.2014.06.116

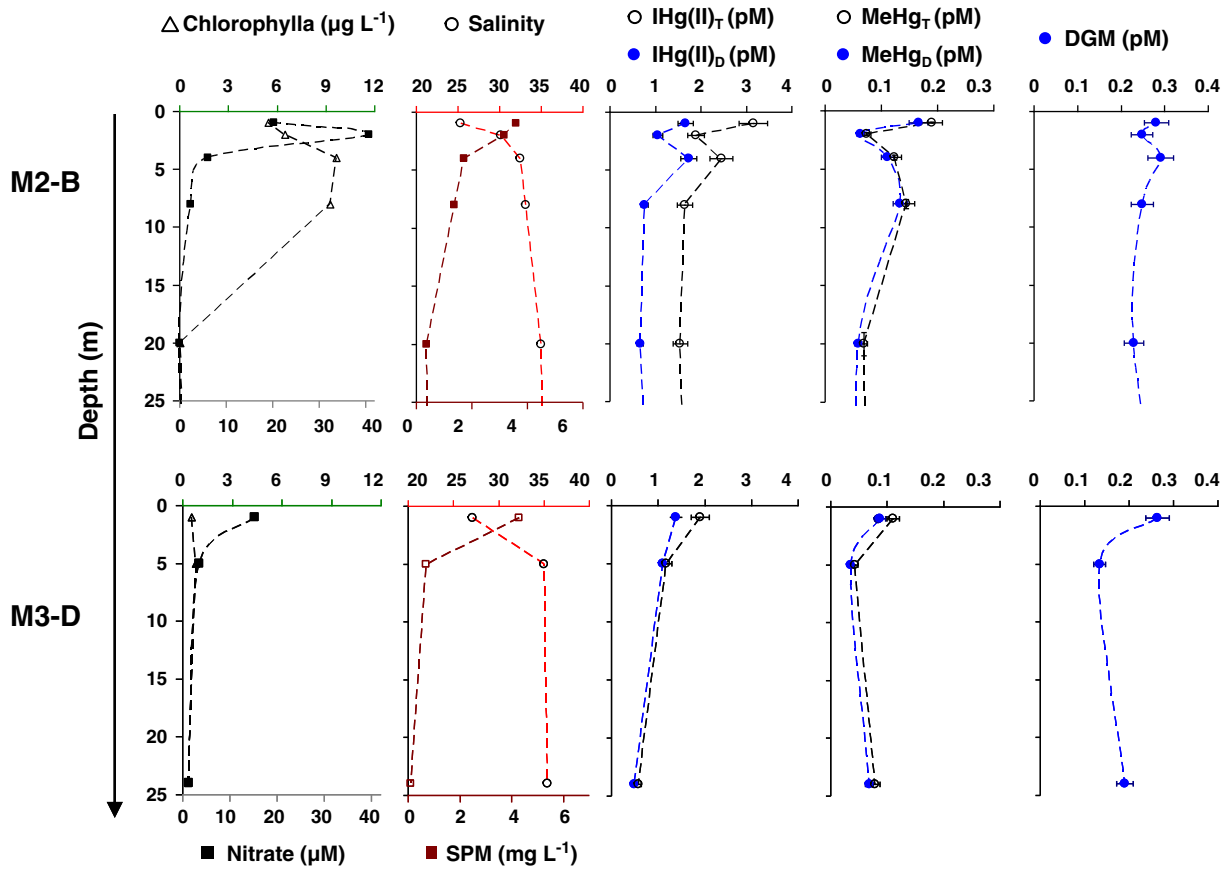

Fig. 4. Depth profiles of salinity, SPM, nitrates, Chlorophyll *a* and Hg species concentrations for two selected stations (M2-B and M3-D) situated in the concentrated plume area. (Error bars represent ± standard deviation).

different experimental conditions (among all stations) and incubation stations (among all conditions) over the two campaigns. For methylation incubations, no significant difference was found between conditions ($p = 0.58$), while a significant higher methylation difference was found for station M2-B among all other stations from campaign M3-0510 ($P < 0.05$).

The ranges of MeHg oxidative demethylation yields were relatively similar between the two campaigns, from 6.1–50.2 and from 2.3–55.3% day^{-1} for M2-0407 and M3-0510, respectively (Table 3). During M2-0407, the highest values were recorded at the near shore station (M2-A) for unfiltered waters under light conditions (50.2% day^{-1}). The yields were roughly reduced by 50% if the waters were filtered or incubated in the dark. At the concentrated plume station (M2-B), similar demethylation yields (18–19% day^{-1}) were found in bulk waters incubated in presence or absence of light. Filtered waters exposed to light returned similar values (15.4% day^{-1}) while dark incubations were lower (6.1% day^{-1}). Similar trends were observed at the marine station (M2-C), where the demethylation yields found in bulk waters incubated under both light and dark conditions were not very different, ranging respectively from 31.7 ± 6.1–20.8 ± 9.3% day^{-1}, while those found in filtered waters exhibit a larger effect of light. During M3-0510, the highest demethylation yields were also found at the near shore station (M3-D, concentrated plume) for both filtered and unfiltered waters under light conditions, 55.3 ± 35.0 and 45.5 ± 12.1% day^{-1}, respectively. The demethylation process was, in both cases, inhibited under dark condition (2.9–22.1% day^{-1}). For the diluted

Table 3
Methylation, demethylation and reduction potentials (mean ± SD, n = 3) in filtered and unfiltered surface waters performed under light and dark conditions for both campaigns: M2-0407 (M2-a, M2-B, M2-C) and M3-0510 (M3-D, M3-E, M3-F). Detection limits are 0.01, 2.0 and 0.3% for methylation, demethylation and reduction yields, respectively.

	Hg(II) Methylation (% day^{-1})				MeHg Demethylation (% day^{-1})				Hg Reduction (% day^{-1})			
	Unfiltered waters		Filtered waters		Unfiltered waters		Filtered waters		Unfiltered waters		Filtered waters	
Stations	Diurnal	Dark	Diurnal	Dark	Diurnal	Dark	Diurnal	Dark	Diurnal	Dark	Diurnal	Dark
M2-A	<0.01	0.1 ± 0.1	<0.01	<0.01	50.2 ± 13.5	20.5 ± 12.2	25.3 ± 11.4	9.6 ± 3.3	6.5 ± 0.2	8.2 ± 0.8	4.3 ± 2.3	1.6 ± 0.4
M2-B	0.4 ± 0.1	0.1 ± 0.1	0.3 ± 0.1	<0.01	18.8 ± 4.0	18.0 ± 7.3	15.4 ± 2.5	6.1 ± 0.2	4.5 ± 0.5	1.2 ± 0.5	10.5 ± 1.4	0.3 ± 1.4
M2-C	0.1 ± 0.1	<0.01	<0.01	<0.01	31.7 ± 6.1	20.8 ± 9.3	28.5 ± 13.8	13.2 ± 6.1	7.2 ± 0.4	8.5 ± 2.2	9.0 ± 0.5	7.3 ± 1.3
M3-D	<0.01	<0.01	<0.01	<0.01	55.3 ± 35.0	22.1 ± 4.6	45.5 ± 12.1	2.9 ± 1.4	16.8 ± 3.4	14.7 ± 2.9	43.5 ± 8.7	7.2 ± 1.4
M3-E	<0.01	<0.01	<0.01	<0.01	23.5 ± 5.8	6.8 ± 0.9	8.0 ± 1.2	2.3 ± 3.0	19.7 ± 3.9	10.5 ± 2.1	25.0 ± 5.0	9.0 ± 1.8
M3-F	<0.01	<0.01	<0.01	<0.01	6.6 ± 3.5	10.9 ± 3.6	24.3 ± 9.4	<2.0	29.8 ± 6.0	5.0 ± 1.0	10.2 ± 2.0	2.8 ± 0.6

Please cite this article as: Sharif A, et al, Fate of mercury species in the coastal plume of the Adour River estuary (Bay of Biscay, SW France), Sci Total Environ (2014), http://dx.doi.org/10.1016/j.scitotenv.2014.06.116

plume station (M3-E), the highest demethylation yields were also measured in bulk waters exposed to sunlight (23.5 ± 5.8% day^{-1}) and they decreased under dark or filtered conditions (6.8–8.0% day^{-1}). At the coastal marine station (M3-F), the highest demethylation yields were found in filtered waters exposed to sunlight (24.3 ± 9.4% day^{-1}) but significant yields were also observed in unfiltered waters incubated under sunlight (6.6 ±3.5% day^{-1}) or dark (10.9 ± 3.6% day^{-1}) conditions. However, demethylation yields were lower than the detection limit (2.0% day^{-1}) in filtered waters incubated in dark condition. ANOVA results shows that unfiltered waters incubated with light exhibit significantly higher demethylation rates than filtered waters controls in the dark ($p < 0.05$). On the other hand, no significant difference could be established for demethylation among the different stations ($p = 0.19$).

The reduction yields were always above the detection limit (0.3% day^{-1}) but were lower during M2-0407 (range: 0.3–10.5% day^{-1}) than M3-0510 (range: 2.8–43.5% day^{-1}). Indeed such net reduction yields also reflect the opposite oxidation taking place in surface waters. No production of gaseous mercury from the MeHg spike (^{201}MeHg) was detectable during the incubations experiments, showing that reductive demethylation was negligible in these conditions (Rodriguez-Gonzalez et al., 2013). In the near shore station (M2-A), significant reduction yields were found in bulk waters incubated in dark condition (8.2 ± 0.8% day^{-1}), probably due to particulate or associated microorganisms present at this station. At M2-B, the highest yield was on the contrary found in filtered waters exposed to light (10.5 ± 1.4% day^{-1}). For the marine station (M2-C), constant reduction yields (range: 7.2–9.0% day^{-1}) were found in unfiltered and filtered waters incubated under light or dark conditions. During M3-0510, reduction yields found for bulk waters in both concentrated and diluted plume stations (M3-D and M3-E) were similar whatever the conditions, whereas higher values were found in filtered waters exposed to light (43.5 ± 8.7% day^{-1} in M3-D and 25.0 ± 5.0% day^{-1} in M3-E). In the seaward station (M3-F), although higher reduction yields were detected in unfiltered waters (29.8 ± 6.0% day^{-1}), they were not significantly different from those obtained in M3-E. In filtered waters incubated with light significantly lower yields were measured (10.2 ± 2.0% day^{-1}) as for plume stations, showing that particles had still some influence in those coastal waters influenced by the plume. ANOVA results could neither exhibit any significant difference of reduction rates between conditions ($p = 0.12$) or between stations ($p = 0.12$).

4. Discussion

4.1. Hg deliveries and partitioning from the Adour estuary to the coastal zone

The $Hg(II)_T$ concentrations measured in the inner estuary or close to the mouth were higher during M2-0407 (up to 21 pM) than during M3-0510 (up to 7.5 pM) but they were overall comparable to similarly impacted estuarine systems, such as the Rhine Estuary (Tseng, 2000), the Patuxent River (Benoit et al., 1998), the Long Island Sound (Rolfhus and Fitzgerald, 2001). $MeHg_T$ concentrations exhibited an opposite trend (higher during M3-0510) and were similar to the Rhine, another low SPM estuary (Tseng, 2000), but lower than those reported in the Pettaquamscutt Estuary (Mason et al., 1999) or the Patuxent River Estuary (Benoit et al., 1998). Hg species concentrations remained overall higher in the Chesapeake Estuary (Mason et al., 1999), which is much more urbanized and industrialized. Concentrations measured at marine stations were consistent with other coastal zones (e.g. Coquery et al., 1995; Ci et al., 2011). Therefore, the concentration gradients established between the Adour estuary and its adjacent marine waters is likely representative of estuaries showing similar anthropogenic impacts and hydrological characteristic.

The $MeHg_T$ and Hg_T inputs (F, g day^{-1}) from the Adour estuary to the coastal zone influence by the plume waters were estimated by using a simple estuarine chemical mass balance model (Boyle et al., 1974) in order to better constrain the net estuarine load to the coastal plume. Indeed, Fig. 2 shows that both $MeHg_T$ and Hg_T do not present a linear trend along with salinity ($p < 0.05$), thus a simple river discharge evaluation is not applicable. Fluxes were thus computed by multiplying the river discharge (D, m^3 day^{-1}) and the difference between the Hg concentrations (mg L^{-1}) detected in the inner estuary (C_{IE}, salinity ca. 0) and the so called "marine water end-member" of the plume (C_M, salinity ca. 35.5), reflecting thus the most diluted plume waters conditions ,and assuming that both end-members remain at steady state on a daily scale, as shown above in paragraph 2.2.2). With such assumptions, the net flux of Hg compounds can be estimated taking into consideration the estuarine tidal mixing of internal and external estuarine waters during flood and ebb tides, using the following equation:

$$F = D(C_{IE} - C_M) \quad (3)$$

The $MeHg_T$ concentrations used to assess the inputs for M2-0407 and M3-0510 were those corresponding to the inner estuarine and coastal marine "end-members" exhibiting, respectively, 0.24 and 0.62 pM in the inner estuary and 0.09 and 0.16 pM in the marine waters. The estuarine inputs of $MeHg_T$ were thus estimated to be 0.9 ± 0.1 g d^{-1} for M2-0407 and 3.5 ± 0.3 g d^{-1} for M3-0510 (Table 5). The same calculations were applied for $Hg(II)_T$ with concentrations of 13.2 and 6.8 pM in the inner estuary for M2-0407 and M3-0510, respectively; and 2.8 pM in marine waters for both campaigns, leading to $Hg(II)_T$ average inputs of 69.1 ± 53.6 and 33.5 ± 17.0 g d^{-1} for M2-0407 and M3-0510, respectively. (Point, 2004) previously reported that the total MeHg and Hg_T fluxes into the estuary, from the Adour River and various urban effluents, were 3.3 ± 5.2 g d^{-1} and 44.15 ± 28.1 g d^{-1}, respectively. These values are in good agreement although the latter are more reliable since the study covered different hydrological conditions and included more samples. It also confirms that the Adour estuary is a significant source of mercury to the coastal waters. Indeed important inputs of Hg have been further established in shelf and deep sediments from the adjacent area of the Bay of Biscay (Stoichev et al., 2004; RNO, 2005).

The Hg export from the Adour estuary is primarily composed of fine particles enriched in Hg(II) which represent about 80% of the total Hg load for both campaigns (Table 2, inner estuarine stations – IE2&3). Indeed, the particulate fractions accounted for most of the Hg_T in the inner estuary, i.e. 86 and 76% for M2-0407 and M3-0510, respectively but these percentages dropped down to usually less than 50% in the plume waters in both cases. These observations suggest that either some of the Hg bound to particles is lost by sedimentation when estuarine waters flow into the external plume, or that a significant fraction of Hg_P is released into the dissolved phase. Although there is overall a negative trend between the percentage of Hg_P and salinity or SPM (data not shown), the data are highly scattered for both campaigns ($r^2 < 0.4$; $p > 0.05$), suggesting that neither estuarine dilution nor sedimentation are significantly governing particulate Hg distribution. Indeed it has been shown by Stoichev et al. (2004), that sedimentation of fine estuarine particles enriched in Hg is occurring farther to the shelf break and not in near shore waters where plume transport and wind turbulence are efficient. During the transfer along the plume, the nature of OM and the presence of organic ligands are ruling may also play an important role for the control of the Hg(II) partitioning. In the case of MeHg, clear positive relationships were found between $MeHg_D$ and $MeHg_T$ (data not shown, $r^2 = 0.6–0.9$; $p < 0.05$), suggesting redistribution rates were faster than methylation/demethylation rates. Thus, either dissolved or particulate MeHg concentrations can be used to gauge the relative importance of riverine supply versus plume production of MeHg. In this sense, MeHg trend along the estuarine plume do not present any significant production pattern as further demonstrated by the methylation incubation experiments.

Please cite this article as: Sharif A, et al, Fate of mercury species in the coastal plume of the Adour River estuary (Bay of Biscay, SW France), Sci Total Environ (2014), http://dx.doi.org/10.1016/j.scitotenv.2014.06.116

Table 4
Potential daily variations of MeHg and gaseous Hg concentrations in the Adour estuarine plume, calculated using models described in Sections 3.2.2 and 3.2.3.

Stations	Δ[MeHg]		Δ[Hg^0]*	
	pmol m^{-3} d^{-1}	ng m^{-3} d^{-1}	pmol m^{-3} d^{-1}	ng m^{-3} d^{-1}
M2-A concentrated plume	−64 ± 51	−13 ± 10	−55 ± 10	−11 ± 2
M2-B concentrated plume	16 ± 1	3 ± 0	−254 ± 0	−51 ± 0
M2-C diluted plume	−26 ± 7	−5 ± 1	−140 ± 20	−28 ± 4
M3-D concentrated plume	−91 ± 39	−18 ± 8	−174 ± 74	−35 ± 15
M3-E diluted plume	−27 ± 20	−5 ± 4	−261 ± 96	−52 ± 19
M3-F marine water	−21 ± 1	−4 ± 0	−180 ± 19	−36 ± 4

*Clark's model (Clark et al., 1995) for gas exchange and Plume mixed layer depth of 1 m used for Δ[Hg°] calculations.

4.2. Demethylation and reduction control the fate of Hg in the plume waters

4.2.1. Controls on Hg transformations

4.2.1.1. Methylation. Statistically Significant methylation yields (Station M2-B, 0.4% day^{-1}) were only observed during the most productive campaign (M2-0407) exhibiting higher POC and Chl.*a* contents. Under these conditions, unfiltered waters having higher biotic activities seems also to provide higher methylation rates, while this observation remains not statistically significant among other conditions (ANOVA). Anaerobic bacteria, such as SRB, associated to particles were identified in the plume waters during the M3 0510 campaign (Colin et al., in preparation) and likely contributed to the Hg methylation in unfiltered waters. These rates are similar to what has been recently reported in water columns from various environments with yields usually lower than 1% day^{-1} (Bouchet et al., 2013, Eckley and Hintelmann, 2006; Monperrus et al., 2007a, 2007b, Lehnherr et al., 2011, Whalin et al., 2007), supporting the conclusion that in situ methylation in surface coastal waters can be a small, but significant source of MeHg. However, as the method used is probably providing a upper limit for methylation potential in these waters, this results demonstrate that methylation remains low in plume waters in these conditions.

4.2.1.2. Demethylation. Beside such low methylation, high demethylation yields were all significant and show no specific difference whatever the stations or seasons (ANOVA). They were especially significant for unfiltered waters incubated under light conditions involving both biological and photochemical activities, when compared to unfiltered dark controls characterized by inhibited light and biotic induced pathways (ANOVA) The observed demethylation yields (range: 2.3–50.2% day^{-1}) are indeed higher than those reported by Bouchet et al. (2013) for the Arcachon Bay (range: 1.3–11.9% day^{-1}), by Monperrus et al. (2007a) for the Thau Lagoon (range: 1.4–24.5% day^{-1}) or the Mediterranean Sea (range: 2.8–19.1% day^{-1}), but rather similar to those measured in polar marine waters (range: 23.0.–51.0% day^{-1}) (Lehnherr et al., 2011). The highest demethylation yields were usually found under light conditions in agreement with the widely accepted idea that abiotic photodemethylation is the main MeHg sink in surface waters containing a minimal amount of particles (e.g. Black et al., 2012; Lehnherr and St Louis, 2009). This is further confirmed here with the low yields obtained from filtered waters incubated under dark conditions. However, elevated demethylation yield have been recently obtained with anaerobic bacteria during laboratory incubations (Bridou et al., 2011) and the dark controls of unfiltered waters provide an *in situ* confirmation of their importance. The contributions of photochemical and biological processes were thus variable among stations but the latter were always significant in these plume waters containing significant amounts of SPM. Both continental and estuarine anaerobic bacteria, which might be involved in the degradation of MeHg, have also been identified in plume waters (Goni-Urriza et al., 2007; Colin et al., in preparation).

4.2.1.3. Reduction. In filtered waters, reduction seems to be dominated by photochemical reactions induced under light incubations, as given by average values, while ANOVA results do not indicate any statistical significance between conditions. Average values show in general higher reduction rates for M3-0510 than for M2-0407, and could indicate a higher contribution of the seasonal sunlight incidence. The role of photochemical pathways has been widely reported (Amyot et al., 1997; Whalin et al., 2007; Zhang and Lindberg, 2001). However, for unfiltered waters, dark processes often account for most of the reduction observed. Microbial reduction has been previously reported in fresh water column (Siciliano et al., 2002) and may also occur in the plume. These net reduction potentials were also not varying significantly as a function of salinity and among sites in general (ANOVA).

4.2.2. The Adour estuarine plume as a sink of MeHg

A simple model was used to predict the variations of MeHg concentrations in the plume (Δ[MeHg], pmol m^{-3} d^{-1}), as a function of the diurnal methylation and demethylation yields (M and D, d^{-1}) and the average ambient Hg(II) and MeHg concentrations (pM), such as:

$$\Delta[MeHg] = M[Hg(II)]_{ambiant} - D[MeHg]_{ambiant} \quad (4)$$

Table 4 shows that most of the stations behave as a sink of MeHg with variations from + 16 to −91 pmol m^{-3} d^{-1}. The highest loss of MeHg concentrations occurred at the concentrated plume stations (M2-A and M3-D). Averaging these values for concentrated and diluted plume waters, area normalized demethylation rates were obtained assuming an average mixed layer depth of the plume of 1 meter (Table 5). Plume waters depth was estimated based on salinity and temperature vertical profiles showing a sharp stratification ranging

Table 5
Comparisons between estuarine inputs of $MeHg_T$ and Hg_T and integrated demethylation in plume waters and Hg^0 evasion from the plume to the atmosphere. Values in brackets were reported by Point (2004) for the same site.

		Plume surface area	Estuarine input $MeHg_T$	Net MeHg demethylation*	Demethylation loss of $MeHg_T$	Estuarine input Hg_T	Hg^0 Flux density#	Atmospheric evasion of Hg^0
		km^2	(g d^{-1})	ng m^{-2} d^{-1}	g d^{-1}	g d^{-1}	ng m^{-2} d^{-1}	g d^{-1}
M2-0407	Concentrated plume	274		11.2 ± 0.1	3.1 ± 0.04		78.6 ± 48.3	21.6 ± 13.2
	Diluted plume	119		5.2 ± 1.4	0.6 ± 0.2		45.0 ± 1.4	5.4 ± 0.2
	Total plume	393	0.9 ± 0.1 (3.3 ± 5.2)		3.7 ± 0.2	69.1 ± 53.6 (44.4 ± 28.1)		26.9 ± 13.4
M3-0510	Concentrated plume	83		18.2 ± 7.9	1.5 ± 0.6		38.8 ± 19.7	3.2 ± 1.6
	Diluted plume	94		5.4 ± 3.9	0.5 ± 0.4		59.3 ± 22.2	5.6 ± 2.1
	Total plume	177	3.5 ± 0.3 (3.3 ± 5.2)		2.0 ± 1.0	33.5 ± 17.0 (44.4 ± 28.1)		8.8 ± 3.7

* Area normalized demethylation rate assuming an estuarine plume mixed layer depth of 1 m.
\# Hg° evasion calculated using gas exchange model (Clark et al., 1995).

Please cite this article as: Sharif A, et al, Fate of mercury species in the coastal plume of the Adour River estuary (Bay of Biscay, SW France), Sci Total Environ (2014), http://dx.doi.org/10.1016/j.scitotenv.2014.06.116

between 0.5–1.5 m depth (Fig SI-4). In Table 5, the net demethylation integrated over the entire plume has been assessed and compared to the estimated MeHg input from the Adour estuary. Remarkably, and considering the large uncertainty of such basic assessment methods, both MeHg input and demethylation in the plume exhibit values in the same order of magnitude. While MeHg input in the plume (0.9 g.d^{-1}) is significantly lower than demethylation loss in the plume (3.7 g.d^{-1}) during M20407, both MeHg input (3.5 g.d^{-1}) and demethylation loss (2.0 g.d^{-1}) are rather balanced during M3-0510. Those results demonstrate that MeHg derived from the estuary can be efficiently demethylated in the plume waters assuming that the residence time of MeHg in the plume remains on a daily scale (based on tidal cycle measurements, see Fig. 3). During M2-0407 and M3-0510 campaigns, such in situ demethylation within plume waters may have drastically reduced the amount of MeHg finally released into coastal waters. This conclusion should be however balanced by the fact that the contribution of coastal sediments has not been taken into account in our budget. Both strong water stratification of the plume waters and previous finding in shore and coastal sediments (Stoichev et al., 2004) showed that little sediment re-suspension is occurring during the investigated campaigns and rather low Hg inputs taking place in such coarse sediments. This suggests that the potential input of Hg species from coastal sediments to the plume waters might be negligible. However this conclusion does not preclude that coastal areas influenced by the plume are not a potential source of MeHg to the marine ecosystem. Overall, these findings strongly suggest, that in such coastal environment, a significant fraction of the estuarine MeHg inputs are degraded in plume waters.

4.2.3. Evasion of Hg^0 from the Adour estuarine plume

Another simple model was used to predict the variations of Hg^0 in the plume and evaluate if the plume is a source of Hg^0 to the atmosphere.

$$\Delta[Hg^o] = R[Hg(II)]_{ambiant} - (k/MLD)[DGM]_{ambiant} \quad (5)$$

where $\Delta[Hg^0]$ is a daily variation of gaseous mercury concentration (pmol m^{-3} d^{-1}), R is the diurnal reduction yield (d^{-1}) averaged from triplicate incubations and k the gas transfer velocity (m d^{-1}) provided by the gas exchange model presented before; MLD is the plume Mixed Layer Depth (m), [Hg(II)] and [DGM] are average natural inorganic mercury and dissolved gaseous mercury concentration (pM). In this model the contribution of TGM in air (see Eq. (1) – Section 2.4.3) has been neglected since DGM is always supersaturated and because only TGM data were available for the first campaign. This approximation was estimated to generate a positive bias averaging 10 and 15% for M2-0407 and M3-0510, respectively, thus much lower to the uncertainty inherent to the air-sea gas exchange model to compute the gas transfer velocity (Sharif et al., 2013). The effective plume's MLD has also been delimited to 1 m, as previously explained in this work. This establishes an approximate boundary diffusion layer of Hg^0, even if plume waters can be mixed down to 5 m depth after strong wind events (Fig SI-4).

All stations exhibited negative variations of Hg^0 (Table 4), ranging from −55 to −261 pmol m^{-3} d^{-1}, which demonstrated that Hg^0 evasion may represent a significant sink of Hg_T for the plume waters. Based on our dataset, the average evasion fluxes of Hg^0 during both M2-0407 and M3-0510 were also estimated using gas exchange models (see Eqs. (1) and (2) – Section 2.4.3) to be 41.2 ± 9.9 ng m^{-2} d^{-1} (range: 29.9-48.7 ng m^{-2} d^{-1}) and 61.3 ± 23.6 ng m^{-2} d^{-1} (range: 38.8–85.8 ng m^{-2} d^{-1}), respectively. These values are similar to previous results obtained using the same approach (gas exchange model) for the Arcachon Bay with 53–241 ng m^{-2} d^{-1}, the Rhine estuary with 33.6–231 ng m^{-2} d^{-1} (Sharif et al., 2013) and for the Irish west coast with 10–144 ng m^{-2} d^{-1} (Gårdfeldt et al., 2003). Finally, the Hg_T estuarine inputs have been compared with the Hg^0 evasion from the plume to the atmosphere (Table 5). On average, the Hg^0 evasion could represent 39% for M2-0407 and 26% for M3-0510 of the total Hg inputs from the estuary. The contributions of the concentrated and diluted plumes were opposite for each campaign, owing to their differences in surface areas and flux densities. However, these findings demonstrate that Hg^0 evasion from plume waters may limit the inputs of Hg_T to the coastal zone. This is likely to be true for other similar estuaries, even if the fate of the evaded Hg^0 should be further evaluated, especially towards its potential re-deposition.

Acknowledgements

The authors would like to thank the European Community, the Aquitaine Region, the Agence Nationale de la Recherche (ANR CESA Program, IDEA project) and the Centre National de la Recherche Scientifique (C.N.R.S.) for their financial support of the different sampling campaigns and analyses. Authors gratefully thank Dr. C. Petus, Prof. P. Anschutz and Dr. H. Etcheber (EPOC UMR 5802, CNRS, Univ. Bordeaux 1, France), N. Duong Thanh (IMER, Vietnam Academy of Science and Technology, Haiphong, Vietnam), and also Captain and crew members of R/V Côte de la Manche (CNRS/INSU) for their helpful assistance for sampling and analyses. A. SHARIF thanks the Libyan Ministry of Higher Education for his doctoral fellowship (ED211, UPPA). This work is a contribution to the Réseau de Recherche Littoral Aquitaine (RRLA/CRA) and the Programme National Environnement Côtier (PNEC/EC2CO).

Appendix A. Supplementary data

Supplementary data to this article can be found online at http://dx.doi.org/10.1016/j.scitotenv.2014.06.116.

References

Amouroux D, Tessier E, Pécheyran C, Donard OFX. Sampling and probing volatile metal(loid) species in natural waters by in-situ purge and cryogenic trapping followed by gas chromatography and inductively coupled plasma mass spectrometry (P-CT-GC-ICP/MS). Anal Chim Acta 1998;377:241–54.

Amyot M, Mierle G, Lean D, Mc Queen DJ. Effect of solar radiation on the formation of dissolved gaseous mercury in temperate lakes. Geochim Cosmochim Acta 1997;61:975–87.

Arleny I, Tabouret H, Rodriguez Gonzalez P, Bareille G, Donard OFX, Amouroux D. Methylmercury bioconcentration in muscle tissue of the European eel (*Anguilla anguilla*) from the Adour estuary (Bay of Biscay, France). Mar Pollut Bull 2007;54:1031–6.

Balcom PH, Hammerschmidt CR, Fitzgerald WF, Lamborg CH, O'Connor JS. Seasonal distributions and cycling of mercury and methylmercury in the waters of New York/New Jersey Harbor Estuary. Mar Chem 2008;109:1–17.

Benoit JM, Gilmour CC, Mason RP, Riedel GS, Riedel GF. Behavior of mercury in the Patuxent River estuary. Biogeochemistry 1998;40:249–65.

Black FJ, Poulin BA, Flegal AR. Factors controlling the abiotic photo-degradation of monomethylmercury in surface waters. Geochim Cosmochim Acta 2012;84:492–507.

Bloom N, Fitzgerald WF. Determination of volatile mercury species at the picogram level by low-temperature gas chromatography with cold-vapour atomic fluorescence detection. Anal Chim Acta 1988;208:151–61.

Bouchet S, Amouroux D, Rodriguez-Gonzalez P, Tessier E, Monperrus M, Thouzeau G, et al. MMHg production and export from intertidal sediments to the water column of a tidal lagoon (Arcachon Bay, France). Biogeochemistry 2013;114:341–58.

Bouchet S, Tessier E, Monperrus M, Bridou R, Clavier J, Thouzeau G, et al. Measurements of gaseous mercury exchanges at the sediment-water, water-atmosphere and sediment-atmosphere interfaces of a tidal environment (Arcachon Bay, France). J Environ Monit 2011;13:1351–9.

Boyle EA, Collier R, Dengler AT, Edmond JM, Ng AC, Stallard RF. On the chemical mass balance in estuaries. Geochim Cosmochim Acta 1974;38:1719–28.

Bridou R, Monperrus M, Gonzalez PR, Guyoneaud R, Amouroux D. Simultaneous determination of mercury methylation and demethylation capacities of various sulfate-reducing bacteria using species-specific isotopic tracers. Environ Toxicol Chem 2011;30:337–44.

Chen B, Wang T, Yin Y, He B, Jiang G. Methylation of inorganic mercury by methylcobalamin in aquatic systems. Appl Organomet Chem 2007;21:462–7.

Choe K-Y, Gill GA, Lehman R. Distribution of particulate, colloidal, and dissolved mercury in San Francisco Bay estuary. 1. Total mercury. Limnol Oceanogr 2003;48:1535–46.

Ci Z, Zhang X, Wang Z, Niu Z. Phase speciation of mercury (Hg) in coastal water of the Yellow Sea, China. Mar Chem 2011;126:250–5.

Clark JF, Schlosser P, Simpson HJ, Stute M, Wanninkhof R, Ho DT. Relationship between gas transfer velocities and wind speeds in the tidal Hudson River determined by the dual tracer technique. In: Jähne E Monahan, editor. Air-water gas transfer. Hanau: Aeon Verlag; 1995. p. 175–800.

Conaway CH, Squire S, Mason RP, Flegal AR. Mercury speciation in the San Francisco Bay estuary. Mar Chem 2003;80:199–225.

Coquery M, Cossa D. Mercury speciation in surface waters of the north sea. Neth J Sea Res 1995;34:245–57.

Coquery M, Cossa D, Martin JM. The distribution of dissolved and particulate mercury in three Siberian estuaries and adjacent Arctic coastal waters. Water Air Soil Pollut 1995;80:653–64.

Cossa D, Heimbürger L-E, Lannuzel D, Rintoul SR, Butler ECV, Bowie AR, et al. Mercury in the Southern Ocean. Geochim Cosmochim Acta 2011;75:4037–52.

Deborde J, Anschutz P, Auby I, Glé C, Commarieu M-V, Maurer D, et al. Role of tidal pumping on nutrient cycling in a temperate lagoon (Arcachon Bay, France). Mar Chem 2008;109:98–114.

Dittman JA, Shanley JB, Driscoll CT, Aiken GR, Chalmers AT, Towse JE, et al. Mercury dynamics in relation to dissolved organic carbon concentration and quality during high flow events in three northeastern U.S. streams. Water Resour Res 2010;46: W07522.

Eckley CS, Hintelmann H. Determination of mercury methylation potentials in the water column of lakes across Canada. Sci Total Environ 2006;368:111–25.

Fitzgerald WF, Lamborg CH. Hammerschmidt. CR. Marine biogeochemical cycling of mercury. Chem Rev 2007;107:641–62.

Gårdfeldt K, Sommar J, Ferrara R, Ceccarini C, Lanzillotta E, Munthe J, et al. Evasion of mercury from coastal and open waters of the Atlantic Ocean and the Mediterranean Sea. Atmos Environ 2003;37:73–84.

Goni-Urriza S, Point D, Amouroux D, Guyoneaud R, Donard OFX, Caumette P, et al. Bacterial community structure along the Adour Estuary (French Atlantic Coast): influence of salinity gradient versus metal contamination. Aquat Microb Ecol 2007;49:47–56.

Hall POJ, Aller RC. Rapid, small-volume, flow injection analysis for $\sum$ CO2 and $NH4^+$ in marine and freshwaters. Limnol Oceanogr 1992;37:1113–9.

Heyes A, Mason RP, Kim E-H, Sunderland E. Mercury methylation in estuaries: Insights from using measuring rates using stable mercury isotopes. Mar Chem 2006;102: 134–47.

Kotnik J, Horvat M, Tessier E, Ogrinc N, Monperrus M, Amouroux D, et al. Mercury speciation in surface and deep waters of the Mediterranean Sea. Mar Chem 2007;107:13–30.

Lehnherr I, St Louis VL. Importance of ultraviolet radiation in the photodemethylation of methylmercury in freshwater ecosystems. Environ Sci Technol 2009;43:5692–8.

Lehnherr I, St. Louis VL, Hintelmann H, Kirk JL. Methylation of inorganic mercury in polar marine waters. Nat Geosci 2011;4:298–302.

Mason R, Fitzgerald W. Mercury speciation in open ocean waters. Water Air Soil Pollut 1991;56:779–89.

Mason RP, Choi AL, Fitzgerald WF, Hammerschmidt CR, Lamborg CH, Soerensen AL, et al. Mercury biogeochemical cycling in the ocean and policy implications. Environ Res 2012;119:101–17.

Mason RP, Lawson NM, Lawrence AL, Leaner JJ, Lee JG, Sheu G-R. Mercury in the Chesapeake Bay. Mar Chem 1999;65:77–96.

Mason RP, Lawson NM, Sheu GR. Mercury in the Atlantic Ocean: factors controlling air-sea exchange of mercury and its distribution in the upper waters. Deep Sea Res Part II 2001;48:2829–53.

Mason RP, Morel FMM, Hemond HF. The role of microorganisms in elemental mercury formation in natural waters. Water Air Soil Pollut 1995;80:775–87.

Monperrus M, Tessier E, Amouroux D, Leynaert A, Huonnic P, Donard OFX. Mercury methylation, demethylation and reduction rates in coastal and marine surface waters of the Mediterranean Sea. Mar Chem 2007a;107:49–63.

Monperrus M, Tessier E, Point D, Vidimova K, Amouroux D, Guyoneaud R, et al. The biogeochemistry of mercury at the sediment-water interface in the Thau Lagoon. 2. Evaluation of mercury methylation potential in both surface sediment and the water column. Estuar Coast Shelf Sci 2007b;72:485–96.

Monperrus M, Point D, Grall J, Chauvaud L, Amouroux D, Bareille G, et al. Determinaton of metal and organometal trophic bioaccumulation in the benthic macrofauna of the Adour estuary coastal zone (SW France, Bay of Biscay). J Environ Monit 2005;7: 693–700.

Murphy J, Riley JP. A modified single solution method for the determination of phosphate in natural waters. Anal Chim Acta 1962;27:31–6.

Navarro P, Amouroux D, Thanh ND, Rochelle-Newall E, Ouillon S, Arfi R, et al. Fate and tidal transport of butyltin and mercury compounds in the waters of the tropical Bach Dang Estuary (Haiphong, Vietnam). Mar Pollut Bull 2012;64:1789–98.

Petus C, Chust G, Gohin F, Doxaran D, Froidefond J-M, Sagarminaga Y. Estimating turbidity and total suspended matter in the Adour River plume (South Bay of Biscay) using MODIS 250-m imagery. Cont Shelf Res 2010;30:379–92.

Point D. Spéciation et biogéochimie des éléments traces métalliques dans l'estuaire de l'Adour. Pau: Université de Pau et des Pays de l'Adour; 2004 [344 pp.].

Point D, Bareille G, Amouroux D, Etcheber H, Donard OFX. Reactivity, interactions and transport of trace elements, organic carbon and particulate material in a mountain range river system (Adour River, France). J Environ Monit 2007;9:157–67.

Poulain AJ, Amyot M, Findlay D, Telor S, Barkay T, Hintelmann H. Biological and photochemical production of dissolved gaseous mercury in a boreal lake. Limnol Oceanogr 2004;49:2265–75.

RNO. Surveillance du Milieu Marin. Travaux du RNO. Ifremer et Ministère de l'Aménagement du Territoire et de l'Environnement. ISSN 1999;1620–1124.

RNO. Surveillance du Milieu Marin. Travaux du RNO. Ifremer et Ministère de l'Ecologie et du Développement Durable. ISSN 2005;1620–1124.

Rodriguez-Gonzalez P, Bouchet S, Monperrus M, Tessier E, Amouroux D. In situ experiments for element species-specific environmental reactivity of tin and mercury compounds using isotopic tracers and multiple linear regression. Environ Sci Pollut Res 2013;20:1269–80.

Rodríguez Martín-Doimeadios RC, Tessier E, Amouroux D, Guyoneaud R, Duran R, Caumette P, et al. Mercury methylation/demethylation and volatilization pathways in estuarine sediment slurries using species-specific enriched stable isotopes. Mar Chem 2004;90:107–23.

Rolfhus KR, Fitzgerald WF. The evasion and spatial/temporal distribution of mercury species in Long Island Sound, CT-NY. Geochim Cosmochim Acta 2001;65:407–18.

Schäfer J, Castelle S, Blanc G, Dabrin A, Masson M, Lanceleur L, et al. Mercury methylation in the sediments of a macrotidal estuary (Gironde Estuary, south-west France). Estuar Coast Shelf Sci 2010;90:80–92.

Schroeder WH, Keeler G, Kock H, Roussel P, Schneeberger D, Schaedlich F. International field intercomparison of atmospheric mercury measurement methods. Water Air Soil Pollut 1995;80:611–20.

Schuster PF, Shanley JB, Marvin-Dipasquale M, Reddy MM, Aiken GR, Roth DA, et al. Mercury and organic carbon dynamics during runoff episodes from a northeastern USA watershed. Water Air Soil Pollut 2008;187:89–108.

Shanley JB, Alisa Mast M, Campbell DH, Aiken GR, Krabbenhoft DP, Hunt RJ, et al. Comparison of total mercury and methylmercury cycling at five sites using the small watershed approach. Environ Pollut 2008;154:143–54.

Sharif A, Tessier E, Bouchet S, Monperrus M, Pinaly H, Amouroux D. Comparison of different air-water gas exchange models to determine gaseous mercury evasion from different European coastal lagoons and estuaries. Water Air Soil Pollut 2013;224: 1606.

Siciliano SD, O'Driscoll NJ, Lean DRS. Microbial reduction and oxidation of mercury in freshwater lakes. Environ Sci Technol 2002;36:3064–8.

Stoichev T, Amouroux D, Monperrus M, Point D, Tessier E, Bareille G, et al. Mercury in surface waters of a macrotidal urban estuary (River Adour, south-west France). Chem Ecol 2006;22:137–48.

Stoichev T, Amouroux D, Wasserman JC, Point D, De Diego A, Bareille G, et al. Dynamics of mercury species in surface sediments of a macrotidal estuarine-coastal system (Adour River, Bay of Biscay). Estuar Coast Shelf Sci 2004;59:511–21.

Tseng CM. Cycle biogéochimique du mercure dans l'environnement: Développements analytiques et spéciation en milieu estuarien. Pau: Université de Pau et des Pays de l'Adour; 2000 [291 pp.].

Tsui MTK, Blum JD, Finlay JC, Balogh SJ, Kwon SY, Nollet YH. Photodegradation of methylmercury in stream ecosystems. Limnol Oceanogr 2013;58:11–23.

Whalin L, Kim E-H, Mason R. Factors influencing the oxidation, reduction, methylation and demethylation of mercury species in coastal waters. Mar Chem 2007;107: 278–94.

Zhang H, Lindberg SE. Sunlight and iron(III)-induced photochemical production of dissolved gaseous mercury in freshwater. Environ Sci Technol 2001;35:928–35.

Please cite this article as: Sharif A, et al, Fate of mercury species in the coastal plume of the Adour River estuary (Bay of Biscay, SW France), Sci Total Environ (2014), http://dx.doi.org/10.1016/j.scitotenv.2014.06.116